Hindawi
International Journal of Photoenergy
Volume 2018, Article ID 6080432, 8 pages
https://doi.org/10.1155/2018/6080432

*Research Article*

# Photocatalytic Activity of Ag-$TiO_2$ Composites Deposited by Photoreduction under UV Irradiation

**Carlos Díaz-Uribe**,[1] **Jose Viloria**,[1] **Lorraine Cervantes**,[1] **William Vallejo**,[1] **Karen Navarro**,[1,2] **Eduard Romero**,[3] **and Cesar Quiñones**[4]

[1]*Grupo de Fotoquímica y Fotobiología, Universidad del Atlántico, Barranquilla, Colombia*
[2]*Universidad Nacional de Córdoba, Cordoba, Argentina*
[3]*Departamento de Química, Universidad Nacional de Colombia, Bogotá, Colombia*
[4]*Institución Universitaria Politécnico Gran Colombiano, Bogotá, Colombia*

Correspondence should be addressed to Carlos Díaz-Uribe; carlosdiaz@mail.uniatlantico.edu.co

Received 30 April 2018; Revised 29 July 2018; Accepted 23 August 2018; Published 21 October 2018

Academic Editor: Mohammad Muneer



In this work, we synthesized Ag nanoparticles on $TiO_2$ thin films deposited on soda lime glass substrates. Ag nanoparticles were synthesized by photoreduction under UV irradiation silver nitrate solution. X-ray diffraction, Raman spectroscopy, scanning electron microscopy (SEM), and X-ray photoelectron spectroscopy (XPS) measurements were used for physicochemical characterization. The structural study showed that all samples were polycrystalline, main phases were anatase and rutile, and no additional signals were detected after surface modification. Raman spectroscopy suggested that silver aggregates deposited on the $TiO_2$ films could exhibit the surface plasmon resonance (SPR) phenomenon; XPS and SEM analysis confirmed $TiO_2$ film morphological modification after photoreduction process. Photocatalytic degradation of methylene blue (MB) was studied under UV irradiation in aqueous solution, and, besides, pseudo-first-order model was used to obtain kinetic information about photocatalytic degradation. Results indicated that Ag-$TiO_2$ showed an important increase in photocatalytic activity under UV (from 20% to 35%); finally, Ag-$TiO_2$ thin films had $k_{app}$ value $2.4 \times 10^{-3} \pm 0.003\ min^{-1}$ of 1.8 times greater than the $k_{app}$ value $1.3 \times 10^{-4} \pm 0.0004\ min^{-1}$ of $TiO_2$ thin films.

## 1. Introduction

Nowadays, titanium dioxide ($TiO_2$) is one of the most important semiconductors in photocatalytic applications because of its prominent properties (e.g., it is harmful, stable, resistant to photocorrosion, inexpensive, and has high photocatalytic properties in the degradation of different pollutants) [1, 2]. However, despite all their characteristics, $TiO_2$ has three main drawbacks: (a) fast recombination rate of photogenerated electron-hole pair, (b) low quantum yield in the photocatalytic reactions in aqueous solutions, and (c) a high bandgap value (3.2 eV, photocatalytic active only under UV irradiation) [3–5]. Due to energy transfer that must be efficient during electron-hole pair separation, fast recombination of the photogenerated charge pair ($e^-/h^+$) after activation of semiconductor is an important drawback for using titanium dioxide ($TiO_2$) as a photocatalyst, because it inhibits redox processes and reduces strongly photocatalytic efficiency [6–8]. Two strategies have been explored to solve this drawback: (a) $TiO_2$ synthesis methods can be modified and optimized and (b) the $TiO_2$ surface can be modified. $TiO_2$ surface modification by transition metal deposition (e.g., silver, platinum, ruthenium, and palladium) has been reported to decrease the recombination process by forming heterostructures and new interfaces that improve semiconductor photocatalytic properties [9–11]. Noble metal cocatalysts can improve photocatalytic properties of semiconductor because they act as electron traps near to conduction bands and/or they improve surface electron excitation by surface plasmonic resonance [12–14]. Nalbandian et al. fabricated Ag-$TiO_2$ nanofibers by electrospinning, and they showed that the presence of the Ag cocatalyst enhanced reactivity

[15]. Yilmaz et al. deposited photochemically Pd nanoparticles on $TiO_2$ nanorods, and they corroborated that electron transfer between Pd and $TiO_2$ was improved after modification process [16]. Currently, different reports showed advances for the fabrication of Ag/$TiO_2$ nanoheterostructure catalysts (e.g., Ag-modified $TiO_2$ nanoparticles, nanowires, and nanorods) [17, 18]; however, several practical problems arise from the use of powder during the photocatalytic process: (a) separation of insoluble catalyst from suspension is harder, (b) particles in suspensions create aggregates especially at high concentrations, and (c) suspensions are difficult to apply on continuous flow systems. The $TiO_2$ thin film is an efficient alternative to solve these drawbacks.

In this contribution, we evaluate the photocatalytic activity of Ag-$TiO_2$ composite thin films in the degradation of methylene blue as a potential alternative in photocatalysis.

## 2. Experimental

*2.1. Photocatalyst Synthesis.* $TiO_2$ films were deposited on soda lime glass (SLG) by doctor blade method. TiO2-Degussa powder (P25) was used as reagent, and after this process, 1.5 $\mu$m $TiO_2$ thin film thickness was obtained [19]. Silver particle deposition on $TiO_2$ films was carried out by chemical photoreduction: first, $TiO_2$ films were immersed in an aqueous silver nitrate solution ($8.0 \times 10^{-2}$ M) for 30 and 60 minutes; after the photoreduction process, $TiO_2$ film colors changed from white to grayish brown.

*2.2. Photocatalyst Characterization.* We study thin film physicochemical properties through measurements of Raman spectroscopy, X-ray diffraction (XRD), and scanning electronic microscopy (SEM); furthermore, the thickness of the thin films was measured through a Veeco Dektak 150 profilometer. Raman spectra were recorded on DRX Raman microscope with laser at 680 nm; SEM images were carried out using a Cambridge S360 microscope operating at acceleration voltage of 20 kV with a scanned area 11 $\mu$m × 10 $\mu$m, and XRD X-ray diffraction patterns of the samples were recorded in Shimadzu 6000 diffractometer with a source of CuK$\alpha$ radiation ($\lambda$ = 0.15418 nm) in a range diffraction angle 2$\theta$ between 20° and 70°. Finally, XPS measurements were performed on X-ray photoelectronic spectrometer (NAP-XPS; brand Specs) with a PHOIBOS 150 1D-DLD analyzer, using a monochromatic source of Al-$K_\alpha$ (1486.7 eV, 13 kV, 100 W) with energy from the 90 eV for the general spectra and 20 eV for the high-resolution spectra. The step was 1 eV for the general spectra and 0.1 eV for the high spectra. We performed 20 measurement cycles for the high-resolution spectra and 3 for the general spectra.

*2.3. Photocatalytic Activity.* Thin films were immersed in blue methylene solution (10 ppm was used as target solution), and prior to irradiation, the system was magnetically stirred in the dark by 1 hour to ensure the equilibrium of dye adsorption-desorption on thin film surface. The system was irradiated by UV lamp with an emission maximum of 260 nm and power 30 W during 180 minutes. All the tests of catalytic reactivity were carried out in aerobic conditions (magnetically stirred: 150 rpm); the irradiated surface area was 3.0 $cm^2$, and the volume of the suspension was 0.015 l. The incident photon flow per unit volume ($I_o = 1.3 \times 10^{-6}$ Einstein$^*L^{-1}{}^*s^{-1}$; Figure 1) shows a general scheme of photoreactor. We chose methylene blue as the model compound because of, since 2010, International Organization for Standardization (ISO) published standard: 10678:2010, namely, the "Determination of photocatalytic activity of surfaces in an aqueous medium by degradation of methylene blue" [20]. Finally, the concentration of dye was determined by spectrophotometry at $\lambda$ = 665 nm for using calibration curve (correlation coefficient $R$ = 0.998).

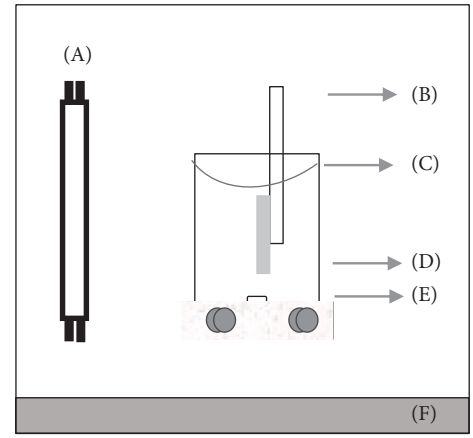


Figure 1: General scheme of photoreactor: (A) UV light source, (B) holder, (C) the beaker container and methylene blue solution, (D) photocatalyst thin film, (E) magnetic stirring, and (F) INOX container.

## 3. Results

*3.1. SEM Analysis.* SEM and EDS were used for morphological compound characterization. Figure 2 shows SEM images for both $TiO_2$ and Ag-$TiO_2$ thin films. Figures 2(a) and 2(b) show that the microaggregates compose $TiO_2$ films: microaggregates have a size range around 50 nm; these results are according to the typical morphology of $TiO_2$-Degussa P25 [21]. Figures 2(c) and 2(d) show the morphological results to Ag-$TiO_2$ thin films; the SEM image allows to differentiate the deposited silver particles. Figure 2 shows the photoreduced particles agglomerated reaching sizes of the order of 200 nm. The EDS analysis showed that the agglomerates observed in the surface of $TiO_2$ corresponded to silver particles (Figures 2(e)).

*3.2. Raman Assay.* Figure 3 shows the Raman spectrum for $TiO_2$ films and the Ag-$TiO_2$ composite thin films deposited after 30 minutes of UV light irradiation. $TiO_2$ films showed characteristic vibration Raman mode signals to anatase phase: signals located at 144 $cm^{-1}$, 398 $cm^{-1}$, and 520 $cm^{-1}$ are assigned to $E_{1g}$ vibration mode, for the signal located at 639 $cm^{-1}$, it is attributed to 398 $cm^{-1}$ $E_{3g}$ vibration mode, and results are according to other reports [22]. Raman

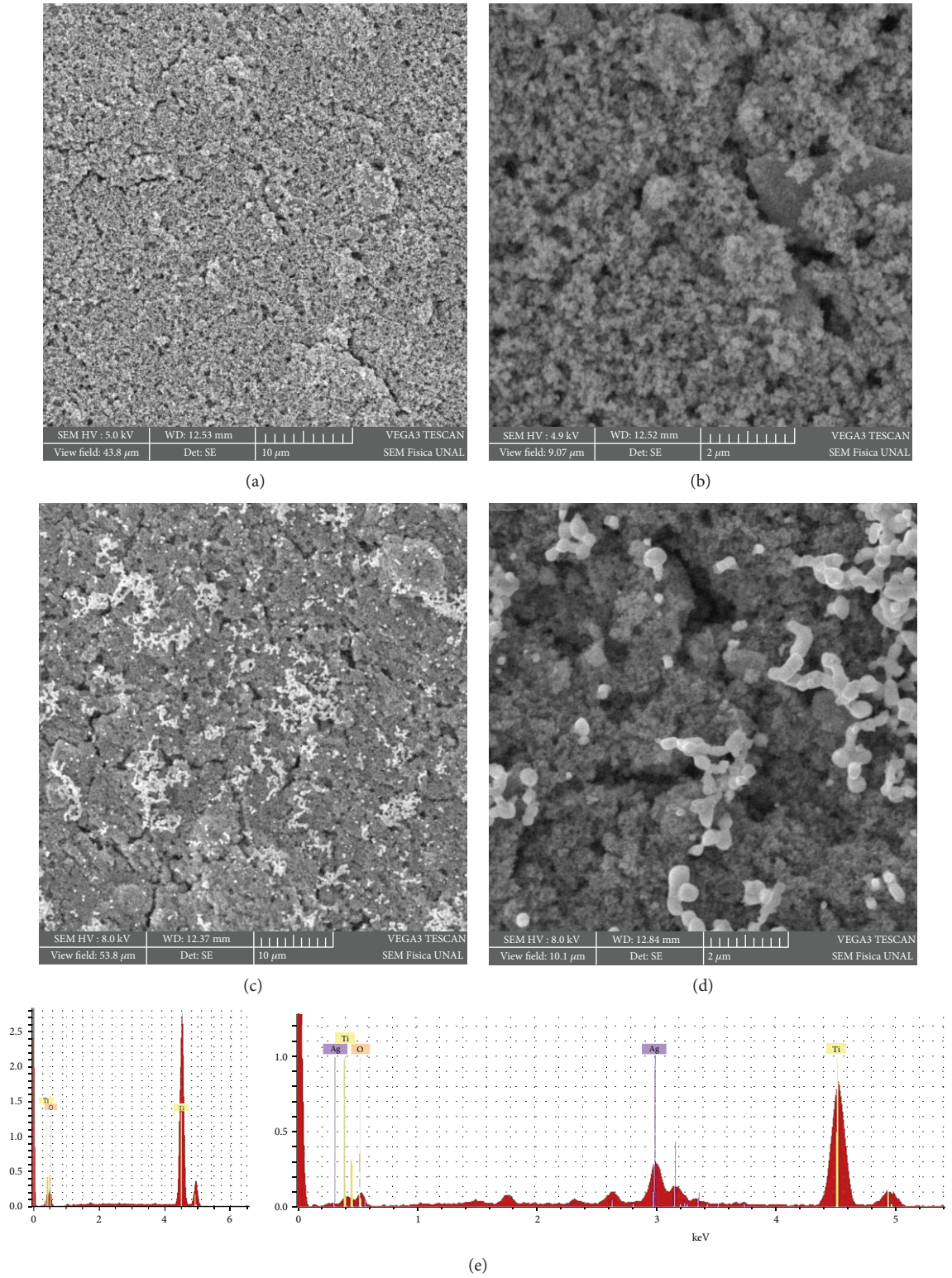


Figure 2: SEM images: (a) $TiO_2$ thin films (10 $\mu$m), (b) $TiO_2$ thin films (2 $\mu$m), (c) Ag-$TiO_2$ (10 $\mu$m), (d) Ag-$TiO_2$ (2 $\mu$m), and (e) $TiO_2$ and Ag-$TiO_2$Ag thin film EDS assay.

spectrum of the modified Ag-$TiO_2$ thin films shows same signals than $TiO_2$ thin films; however, the intensity of all signals is increasing; this behavior is associated to phenomenon known as surface plasmon resonance (SPR). This process is characterized by the increase in several orders of magnitude of the intensity of the signals in the Raman spectrum due to the effect of metal nanometric scale species adsorbed on semiconductor surface [23–25]. Different reports indicated

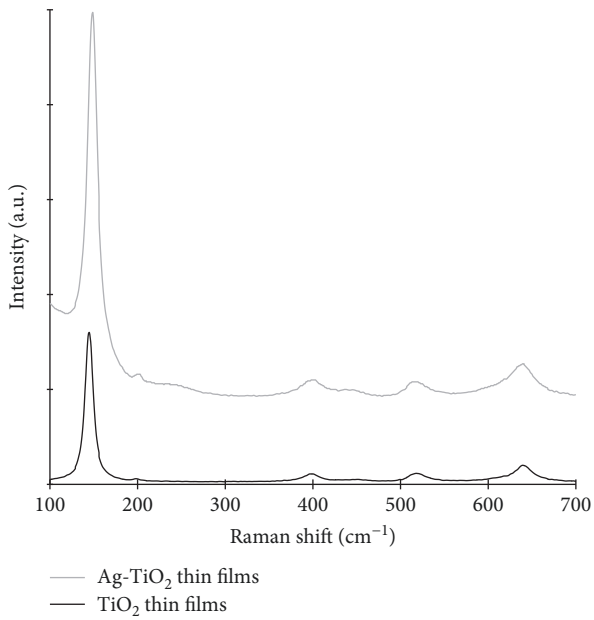


FIGURE 3: Raman spectrum to $TiO_2$ thin films and Ag-$TiO_2$ composite thin films.

that some noble metal nanoparticles (gold, silver, palladium, and platinum) can generate an intense surface plasmon resonance when adsorbed onto semiconductors; finally, SPR process could affect optical, electrical, and photocatalytic properties of $TiO_2$ [26, 27].

*3.3. XRD Assay.* Figure 4 shows the experimental XRD pattern for both $TiO_2$ and Ag-$TiO_2$ thin films. XRD pattern showed peaks at $2\theta = 25.4^\circ$, $2\theta = 38.2^\circ$, $2\theta = 48.2^\circ$, and $2\theta = 62.5^\circ$; they correspond to planes (101), (112), (200), and (204). These signals are typical of the $TiO_2$ anatase phase (JCPDS #071-1166); diffraction pattern also shows additional diffraction signals at $2\theta = 27.8^\circ$ and $2\theta = 55.0^\circ$; these reflections can be associated to the planes (110) and (220) of the rutile crystalline phase (JCPDS #021-1276). The presence of the rutile is due to the composition of the material used as $TiO_2$ source (Degussa P25). Furthermore, after Ag photoreduction on $TiO_2$ surface, the intensity of main signal (located at $2\theta = 25.4^\circ$) decreases indicating that the anchoring process did not change the characteristic crystal surface structure of $TiO_2$; these results are according to SEM assay [28].

*3.4. XPS Assay.* XPS measurements were conducted to verify the surface components and valence states of Ag-$TiO_2$ thin film. Figure 5(a) shows profile XPS spectrum to Ag-$TiO_2$ thin film. The profile of the sample shows the typical signals of binding energy corresponding to Ag, Ti, O, and C elements.

The signals at 574.0 eV, 374.0 eV, and 368.0 eV correspond to the electronic transitions of Ag $3p_{3/2}$, Ag $3d_{3/2}$, and Ag $3d_{3/2}$, respectively; Figure 5(c) plots the HRXPS spectrum of Ag $3d_{5/2}$ and Ag $3d_{3/2}$ double peaks, which are centered at 367.8 and 373.8 eV, respectively; and the splitting of the 3d doublet was 6.0 eV. This binding energy indicated that silver was of metallic nature. These results are according to other reports [29–31]. Figure 5(b) shows the peaks at 458.6 and 464.3 eV; these signals correspond to Ti $2p_{3/2}$ and Ti $2p_{1/2}$ indicating the formation of $Ti^{4+}$ in $TiO_2$ [32–34]. Figure 5(a) also shows an important signal at 530.2 eV, and this corresponds to the phototransition O1s; finally, the signal located at 285 eV corresponds to electronic transition of C 1s. This signal is typical of atmospheric $CO_2$ absorbed on the surface of the simple.

We performed quantitative assay of Ag-$TiO_2$ thin films for using XPS survey spectra shown in Figure 5; it mainly consists in determination of the relative concentration of respective surface atoms like Ti, O, C, and Ag as follows:

$$n_i = \frac{(I_i/\mathrm{ASF}_i)}{\sum_i^n (I_i/\mathrm{ASF}_i)}, \tag{1}$$

where $I_i$ corresponds to relative intensity height of the $O_{1s}$, $Ti_{2p}$, $Ag_{3d}$, and $C_{1s}$ core-level line peaks and $\mathrm{ASF}_i$ is the atomic sensitivity factors related to the height of specific peaks [35–37]. Table 1 summarizes the corresponding partial concentration of specific elements in the Ag-$TiO_2$ thin films.

*3.5. Photocatalytic Assay.* Figure 6 shows the $C_t/C_o$ (methylene blue) as a function of time under UV irradiation, in the presence of $TiO_2$ and Ag-$TiO_2$ thin films for 180 min. Figure 6 shows similar profile to behavior observed for the photocatalytic degradation of different dyes; previous studies showed that photocatalytic degradation rate of textile dyes in heterogeneous photocatalytic oxidation systems under UV light illumination followed Langmuir–Hinshelwood (L–H); the Langmuir–Hinshelwood expression that explains the kinetics of heterogeneous catalytic systems is given by [38–44]

$$r = -\frac{dC}{dt} = \frac{k_t K[C]}{1 + K[C]}, \tag{2}$$

where $r$ is the rate of dye mineralization, $k_t$ is the rate constant, $[C]$ is the methylene blue concentration, and $K$ is the adsorption coefficient. Equation (1) can be solved explicitly for $(t)$ by using discrete changes in [MB] from the initial concentration to a zero reference point; however, when the concentration of substrate is in the scale of $\mu$moles, an apparent first-order model can be assumed; in our case,

$$r = -\frac{dC}{dt} = k_t K[C]. \tag{3}$$

Integration of (2):

$$\begin{aligned} [C] &= [C]_o e^{-k_{\mathrm{app}} * t}, \\ \ln\left(\frac{[C]_t}{[C]_o}\right) &= -k_{\mathrm{app}} * t, \end{aligned} \tag{4}$$

where $(t)$ represents time in minutes, $k_{\mathrm{app}}$ $(k_t K)$ is the apparent reaction rate constant ($\mathrm{min}^{-1}$), and $[C]_t$ is the

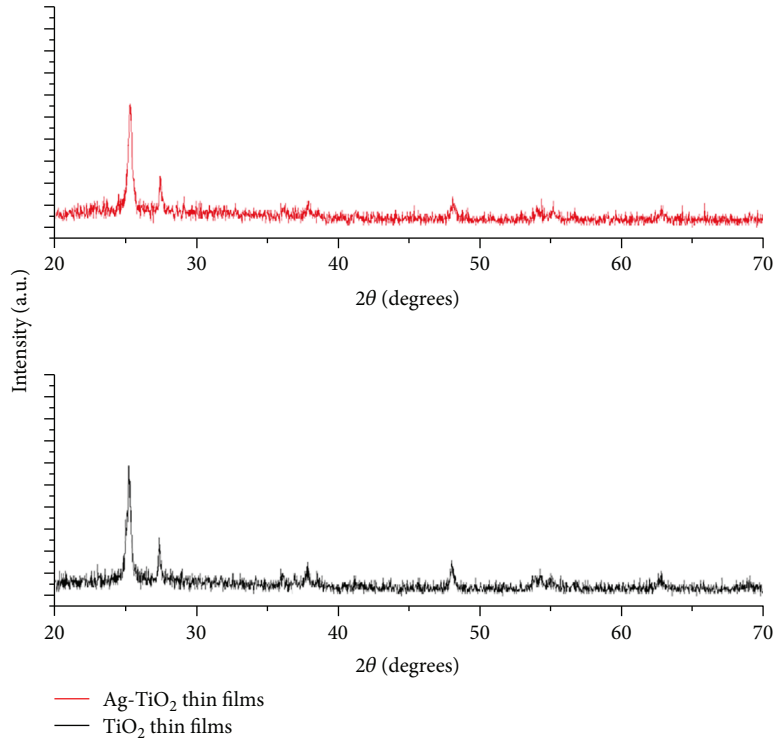


Figure 4: XRD pattern for both $TiO_2$ and Ag-$TiO_2$ thin films.

concentration of MB at each time. (L–H) kinetics is commonly used to explain the kinetics of the heterogeneous catalytic processes; the assumption of a pseudo-first-order kinetic model was used in several studies to characterize the effect of different experimental conditions [45–47]. Figure 6 shows that when the MB solution was exposed to UV radiation on $TiO_2$ thin films, a small reduction in the concentration of MB was observed (near 20%). These results are according to expected because $TiO_2$ thin films are photocatalytic active under this kind of radiation. Visible is a typical behavior for $TiO_2$ due to their well-known wide bandgap value [48].

Furthermore, Figure 6 shows that Ag-$TiO_2$ thin films showed an important increase in the photocatalytic activity under UV (near 35%); these results could be due to the silver aggregates deposited on the $TiO_2$ surface that can accumulate charge and accept electrons inside the semiconductor. The accumulation of electrons can reduce the carrier's recombination increasing generation of reactive oxygen species, and besides, Ag particle on $TiO_2$ can change and a collective oscillation can be generated, which is known as localized surface plasmon resonance (SPR) [49]; according to other reports, silver particles exhibit collective oscillation of their electrons in the conduction band, and it is suggested that the association between the semiconductor and the metal can increase photocatalytic activity, which coincides with the results obtained in this work [50]. Pseudo-first-order model was applied to kinetic data of Figure 6. The $k_{app}$ values for each test were determined from the slope of the linear fitting of $\ln(C_t/C_o)$ vs time (Figure 7).

Ag-$TiO_2$ thin films had a $k_{app}$ value $2.4 \times 10^{-3}\,\text{min}^{-1}$; this value was 1.8 times greater than the $k_{app}$ value $1.3 \times 10^{-4}\,\text{min}^{-1}$ of $TiO_2$ thin films. $k_{app}$ values confirmed that the photoreduction process was effective and demonstrated that this method could be used as an alternative to increasing the photocatalytic activity of $TiO_2$ under UV light irradiation. We reported in a previous work that Ag-$TiO_2$ thin films had antimicrobial activity against *Staphylococcus aureus*; same material demonstrated both photocatalytic and antimicrobial activities [51]. Reactive oxygen species generated in advance oxidation process are endogenous, highly reactive, oxygen molecules, and these species can originate oxidation reactions of many organic and biological compounds (e.g., singlet oxygen and oxygen free radicals such as hydroxyl radical, superoxide anion, hydroperoxyl ($HOO^{\cdot}$), or other similar radicals); our results corroborate high reactivity of these chemical species [52].

## 4. Conclusions

In this work, we deposited Ag microaggregates on $TiO_2$ thin films. SEM characterization demonstrated microaggregate formation on $TiO_2$ surface, and besides, Raman spectroscopy indicated that surface modification generated SPR process; furthermore, XRD assay indicated that all thin films were crystalline and XPS assay indicates that silver was of metallic nature after photoreduction on $TiO_2$ thin films. Photocatalytic activity of Ag-$TiO_2$ thin films was higher than that of $TiO_2$ thin films; kinetic results showed that the $k_{app}$ for

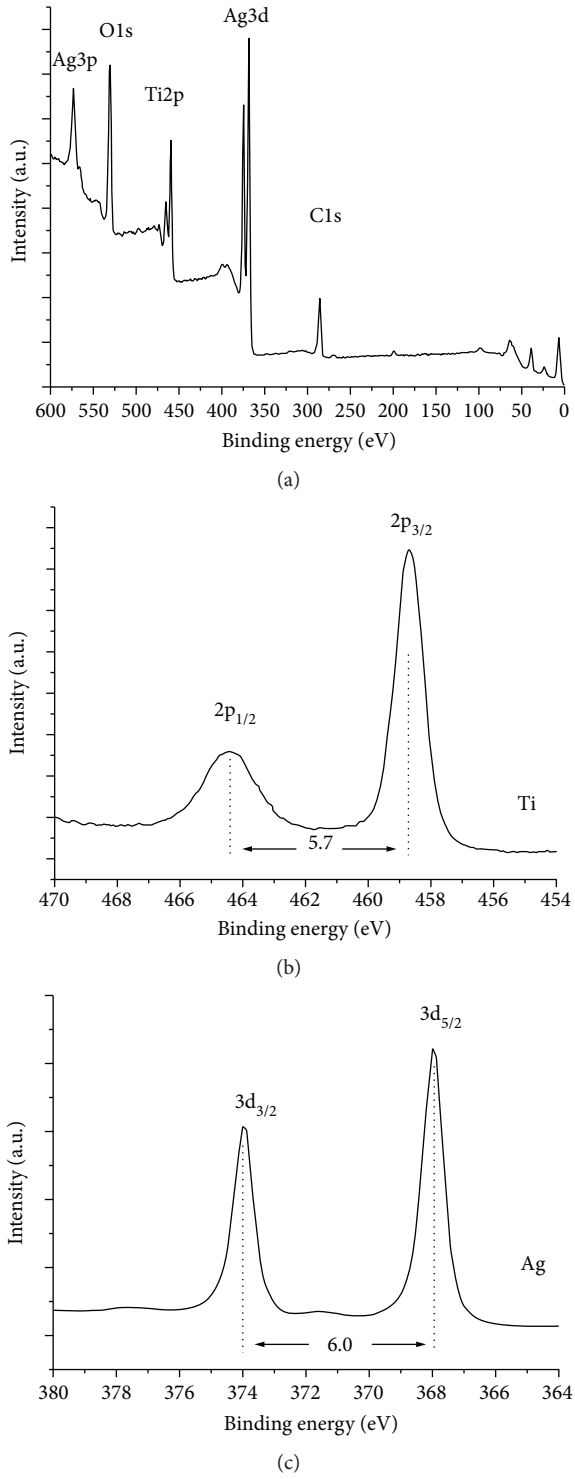


Figure 5: (a) XPS spectrum to Ag-$TiO_2$ thin films, (b) HRXPS Ti 2p spectrum to Ag-$TiO_2$ thin films, and (c) HRXPS Ag 3d spectrum to Ag-$TiO_2$ thin films. All binding energies of the XPS spectra are calibrated with reference to the C1s peak at 285 eV.

Table 1: Partial concentration for elements of Ag-$TiO_2$ thin films.

| Element | Oxygen | Titanium | Silver | Carbon |
|---|---|---|---|---|
| % | 39.1 | 15.9 | 8.5 | 36.6 |

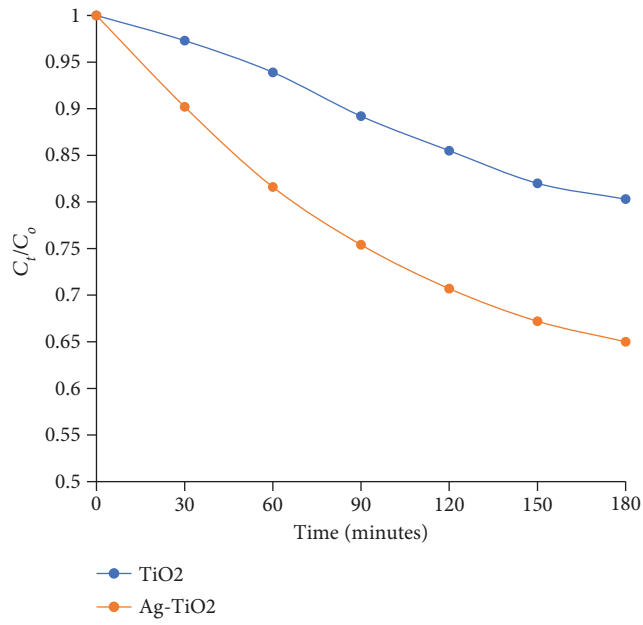


Figure 6: $C_t/C_o$ vs time under UV light irradiation, where $C_t$ refers to the concentration at time $t$ of MB and $C_o$ refers to initial concentration.

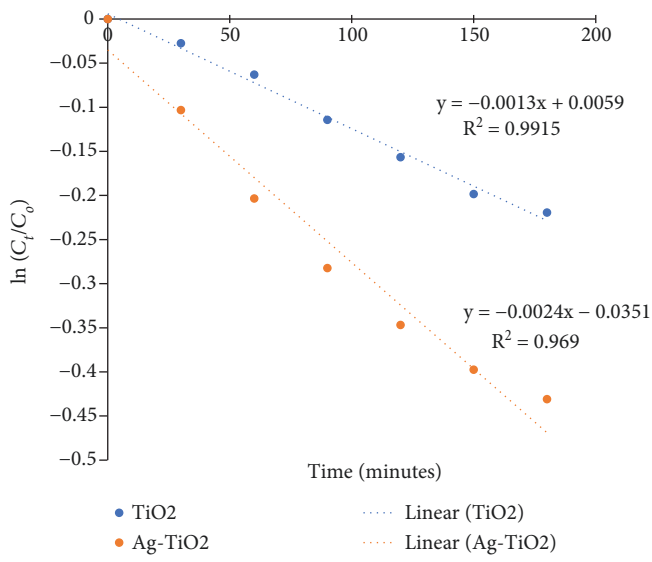


Figure 7: Fitting ln $(C_t/C_o)$ vs $(t)$ for tests, where $C_t$ refers to the concentration of MB at time $(t)$ and $C_o$ refers to the initial concentration of MB; inside figure is the $R$ value and equation of linear fitting.

Ag-$TiO_2$ thin films was greater ($2.4 \times 10^{-3}\,\text{min}^{-1}$) than the $k_{app}$ for $TiO_2$ thin films ($1.3 \times 10^{-3}\,\text{min}^{-1}$).

## Data Availability

The data used to support the findings of this study are available from the corresponding author upon request.

## Conflicts of Interest

The authors declare that they have no conflicts of interest.

## Acknowledgments

This research was supported by Universidad del Atlántico. Furthermore, the authors thank Universidad de Antioquia for supporting the XPS measurements.

## References

[1] J. Schneider, M. Matsuoka, M. Takeuchi et al., "Understanding $TiO_2$ photocatalysis: mechanisms and materials," *Chemical Reviews*, vol. 114, no. 19, pp. 9919–9986, 2014.

[2] M. J. G azquez, J. P. Bolívar, R. Garcia-Tenorio, and F. Vaca, "A review of the production cycle of titanium dioxide pigment," *Materials Sciences and Applications*, vol. 5, no. 7, pp. 441–458, 2014.

[3] Y. Du and J. Rabani, "The measure of $TiO_2$ photocatalytic efficiency and the comparison of different photocatalytic titania," *The Journal of Physical Chemistry. B*, vol. 107, no. 43, pp. 11970–11978, 2003.

[4] C. Ming, Y. Ku, F. Tien, and Y. L. Kuo, "Effect of platinum on the decomposition efficiency and apparent quantum yield of photocatalysis of isopropanol in an annular photoreactor," *Journal of Advanced Oxidation Technologies*, vol. 10, no. 2, pp. 36–368, 2007.

[5] B. Kılıç, N. Gedik, S. Pıravadıllı, A. Serhan, and E. Gürd, "Band gap engineering and modifying surface of $TiO_2$ nanostructures by $Fe_2O_3$ for enhanced-performance of dye sensitized solar cell," *Materials Science in Semiconductor Processing*, vol. 31, pp. 363–371, 2015.

[6] P. Zawadzki, A. B. Laursen, K. W. Jacobsen, S. Dahl, and J. Rossmeisl, "Oxidative trends of $TiO_2$ – hole trapping at anatase and rutile surfaces," *Energy & Environmental Science*, vol. 5, no. 12, pp. 9866–9869, 2012.

[7] L. Cavigli, F. Bogani, A. Vinattieri et al., "Carrier recombination dynamics in anatase $TiO_2$ nanoparticles," *Solid State Sciences*, vol. 12, no. 11, pp. 1877–1880, 2010.

[8] D. Punnoose, C. H. S. S. Pavan, H. Woong et al., "Reduced recombination with an optimized barrier layer on $TiO_2$ in PbS/CdS core shell quantum dot sensitized solar cells," *New Journal of Chemistry*, vol. 40, no. 4, pp. 3423–3431, 2016.

[9] N. Rahimi, R. A. Pax, and E. M. Gray, *Progress in Solid State Chemistry*, vol. 44, no. 3, pp. 86–105, 2016.

[10] A. Bumajdad and M. Madkour, "Understanding the superior photocatalytic activity of noble metals modified titania under UV and visible light irradiation," *Physical Chemistry Chemical Physics*, vol. 16, no. 16, pp. 7146–7158, 2014.

[11] J. Choi, H. Park, and M. R. Hoffmann, "Effects of single metal-ion doping on the visible-light photoreactivity of $TiO_2$," *The Journal of Physical Chemistry C*, vol. 114, no. 2, pp. 783–792, 2009.

[12] M. Kotesh, K. Bhavani, G. Naresh, B. Srinivas, and A. Venugopala, "Plasmonic resonance nature of Ag-Cu/$TiO_2$ photocatalyst under solar and artificial light: synthesis, characterization and evaluation of $H_2O$ splitting activity," *Applied Catalysis B: Environmental*, vol. 199, pp. 282–291, 2016.

[13] S. Shuang, R. Lv, Z. Xie, and Z. Zhang, "Surface plasmon enhanced photocatalysis of Au/Pt-decorated $TiO_2$ nanopillar arrays," *Scientific Reports*, vol. 6, pp. 1–8, 2016.

[14] S. Kochuveedu, D. Kim, and D. Ha Kim, "Surface-plasmon-induced visible light photocatalytic activity of $TiO_2$ nanospheres decorated by Au nanoparticles with controlled configuration," *The Journal of Physical Chemistry C*, vol. 116, no. 3, pp. 2500–2506, 2012.

[15] M. J. Nalbandian, M. Zhang, J. Sanchez et al., "Synthesis and optimization of Ag–$TiO_2$ composite nanofibers for photocatalytic treatment of impaired water sources," *Journal of Hazardous Materials*, vol. 299, pp. 141–148, 2015.

[16] P. Yilmaz, A. Lacerda, I. Larrosa, and S. Dunn, "Photoelectrocatalysis of rhodamine B and solar hydrogen production by $TiO_2$ and Pd/$TiO_2$ catalyst systems," *Electrochimica Acta*, vol. 231, pp. 641–649, 2017.

[17] C. Su, L. Liu, M. Zhang, Y. Zhanga, and C. Shao, "Fabrication of Ag/$TiO_2$ nanoheterostructures with visible light photocatalytic function via a solvothermal approach," *CrystEngComm*, vol. 14, no. 11, pp. 3989–3999, 2012.

[18] K. Kusdianto, D. Jiang, M. Kubo, and M. Shimada, "Fabrication of $TiO_2$–Ag nanocomposite thin films via one-step gas-phase deposition," *Ceramics International*, vol. 43, no. 6, pp. 5351–5355, 2017.

[19] C. Quiñones, Y. Ayala, and W. Vallejo, "Methylene blue photoelectrodegradation under UV irradiation on Au/Pd-modified $TiO_2$ films," *Applied Surface Science*, vol. 257, no. 2, pp. 367–371, 2010.

[20] A. Mills, "An overview of the methylene blue ISO test for assessing the activities of photocatalytic films," *Applied Catalysis B: Environmental*, vol. 128, pp. 144–149, 2012.

[21] I. Ahmed, Z. Khan, and M. Ali, "Photocatalytic degradation of nitro and chlorophenols using doped and undoped titanium dioxide nanoparticles," *Journal of Nanomaterials*, vol. 2011, Article ID 589185, 8 pages, 2011.

[22] N. Mahdjoub, N. Allen, P. Kelly, and V. Vishnyakov, "SEM and Raman study of thermally treated $TiO_2$ anatase nanopowders: influence of calcination on photocatalytic activity," *Journal of Photochemistry and Photobiology A: Chemistry*, vol. 211, no. 1, pp. 59–64, 2010.

[23] M. Torrell, R. Kabir, L. Cunha et al., "Tuning of the surface plasmon resonance in $TiO_2$/Au thin films grown by magnetron sputtering: the effect of thermal annealing," *Journal of Applied Physics*, vol. 109, no. 7, article 074310, 2011.

[24] A. Tanaka, S. Sakaguchi, K. Hashimoto, and H. Kominami, "Preparation of Au/$TiO_2$ with metal cocatalysts exhibiting strong surface plasmon resonance effective for photoinduced hydrogen formation under irradiation of visible light," *ACS Catalysis*, vol. 3, no. 1, pp. 79–85, 2013.

[25] A. Tanaka, K. Teramura, S. Hosokawa, H. Kominamic, and T. Tanaka, "Visible light-induced water splitting in an aqueous suspension of a plasmonic Au/$TiO_2$ photocatalyst with metal co-catalysts," *Chemical Science*, vol. 8, no. 4, pp. 2574–2580, 2017.

[26] K. H. Leong, H. Y. Chu, S. Ibrahim, and P. Saravanan, "Palladium nanoparticles anchored to anatase $TiO_2$ for enhanced surface plasmon resonance-stimulated, visible-light-driven photocatalytic activity," *Beilstein Journal of Nanotechnology*, vol. 6, pp. 428–437, 2015.

[27] M. Zhou, J. Zhang, B. Cheng, and H. Yu, "Enhancement of visible-light photocatalytic activity of mesoporous Au-$TiO_2$

nanocomposites by surface plasmon resonance," vol. 2012, Article ID 532843, 10 pages, 2012.

[28] Z. Huang, B. Zheng, S. Zhu et al., "Photocatalytic activity of phthalocyanine-sensitized $TiO_2$–$SiO_2$ microparticles irradiated by visible light," *Materials Science in Semiconductor Processing*, vol. 25, pp. 148–152, 2014.

[29] J. Yu, J. Xiong, B. Cheng, and S. Liu, "Fabrication and characterization of Ag–$TiO_2$ multiphase nanocomposite thin films with enhanced photocatalytic activity," *Applied Catalysis B: Environmental*, vol. 60, no. 3-4, pp. 211–221, 2005.

[30] J. F. Moulder, W. F. Stickle, P. E. Sobol, and K. D. Bomben, *Handbook of X-Ray Photoelectron Spectroscopy*, Perkin-Elmer Corporation Physical Electronics Division, 1992.

[31] E. Stathatos and P. Lianos, "Photocatalytically deposited silver nanoparticles on mesoporous $TiO_2$ films," *Langmuir*, vol. 16, no. 5, pp. 2398–2400, 2000.

[32] L. Ma, Y. Huang, M. Hou, Z. Xie, and Z. Zhang, "Ag nanorods coated with ultrathin $TiO_2$ shells as stable and recyclable SERS substrates," *Scientific Reports*, vol. 5, no. 1, article 15442, 2015.

[33] J. Chen, H. Su, X. You, J. Gao, W. M. Lau, and D. Zhang, "3D $TiO_2$ submicrostructures decorated by silver nanoparticles as SERS substrate for organic pollutants detection and degradation," *Materials Research Bulletin*, vol. 49, pp. 560–565, 2014.

[34] B. Erdem, R. A. Hunsicker, G. W. Simmons, E. D. Sudol, V. L. Dimonie, and M. S. El-Aasser, "XPS and FTIR surface characterization of $TiO_2$ particles used in polymer encapsulation," *Langmuir*, vol. 17, no. 9, pp. 2664–2669, 2001.

[35] M. Kwoka, V. Galstyan, E. Comini, and J. Szube, "Pure and highly Nb-doped titanium dioxide nanotubular arrays: characterization of local surface properties," *Nanomaterials*, vol. 7, no. 12, p. 456, 2017.

[36] J. F. Watts and J. Wolstenholme, *An introduction to surface analysis by XPS and AES*, John Wiley & Sons, Ltd, 2003.

[37] J. C. Vickerman and I. S. Gilmore, "Surface analysis—the principal techniques," John Wiley & Sons, Chichester, UK, 2nd edition, 2009.

[38] S. Ghasemi, S. Rahimnejad, S. Rahman Setayesh, M. Hosseini, and M. R. Gholami, "Kinetics investigation of the photocatalytic degradation of acid blue 92 in aqueous solution using nanocrystalline $TiO_2$ prepared in an ionic liquid," *Progress in Reaction Kinetics and Mechanism*, vol. 34, no. 1, pp. 55–76, 2009.

[39] I. Konstantinou and T. Albanis, "$TiO_2$-assisted photocatalytic degradation of azo dyes in aqueous solution: kinetic and mechanistic investigations: a review," *Applied Catalysis B: Environmental*, vol. 49, no. 1, pp. 1–14, 2004.

[40] K. V. Kumar, K. Porkodi, and F. Rocha, "Langmuir–Hinshelwood kinetics – a theoretical study," *Catalysis Communications*, vol. 9, no. 1, pp. 82–84, 2008.

[41] A. R. Khataee, M. Fathinia, and S. Aber, "Kinetic modeling of liquid phase photocatalysis on supported $TiO_2$ nanoparticles in a rectangular flat-plate photoreactor," *Industrial & Engineering Chemistry Research*, vol. 49, no. 24, pp. 12358–12364, 2010.

[42] V. Djokic, J. Vujovic, A. Marinkovic et al., "A study of the photocatalytic degradation of the textile dye CI basic yellow 28 in water using a P160 $TiO_2$-based catalyst," *Journal of the Serbian Chemical Society*, vol. 77, no. 12, pp. 1747–1757, 2012.

[43] L. Elsellami, F. Vocanson, and F. Dappozzeetal, "Kinetic of adsorption and of photocatalytic degradation of phenylalanine effect of pH and light intensity," *Applied Catalysis A: General*, vol. 380, no. 1-2, pp. 142–148, 2010.

[44] N. P. Xekoukoulotakis, C. Drosou, C. Brebou et al., "Kinetics of UV-A/$TiO_2$ photocatalytic degradation and mineralization of the antibiotic sulfamethoxazole in aqueous matrices," *Catalysis Today*, vol. 161, no. 1, pp. 163–168, 2011.

[45] C. S. Turchi and D. Ollis, "Photocatalytic degradation of organic water contaminants: mechanisms involving hydroxyl radical attack," *Journal of Catalysis*, vol. 122, no. 1, pp. 178–192, 1990.

[46] T. Zhang, T. Oyama, A. Aoshima, H. Hidaka, J. Zhao, and N. Serpone, "Photooxidative *N*-demethylation of methylene blue in aqueous $TiO_2$ dispersions under UV irradiation," *Journal of Photochemistry and Photobiology A: Chemistry*, vol. 140, no. 2, pp. 163–172, 2001.

[47] J. W. Rodriguez-Acosta, M. Á. Mueses, and F. Machuca-Martínez, "Mixing rules formulation for a kinetic model of the Langmuir-Hinshelwood semipredictive type applied to the heterogeneous photocatalytic degradation of multicomponent mixtures," *International Journal of Photoenergy*, vol. 2014, Article ID 817538, 9 pages, 2014.

[48] C. Xu, G. P. Rangaiah, and X. S. Zhao, "Photocatalytic degradation of methylene blue by titanium dioxide: experimental and modeling study," *Industrial and Engineering Chemistry Research*, vol. 53, no. 38, pp. 14641–14649, 2014.

[49] P. Liu, P. Zhang, D. Liang, and W. Xue, "Preparation, characterization and photodegradation of methylene blue based on $TiO_2$ microparticles modified with thiophene substituents," *Chinese Science Bulletin*, vol. 57, no. 33, pp. 4381–4386, 2012.

[50] R. S. André, C. A. Zamperini, E. G. Mima et al., "Antimicrobial activity of $TiO_2$: Ag nanocrystalline heterostructures: experimental and theoretical insights," *Chemical Physics*, vol. 459, pp. 87–95, 2015.

[51] W. Vallejo, C. Díaz-Uribe, K. Navarro, R. Valle, J. W. Arboleda, and E. Romero, "Estudio de la actividad antimicrobiana de películas delgadas de dióxido de titanio modificado con plata," *Revista de la Academia Colombiana de Ciencias Exactas, Físicas y Naturales*, vol. 40, no. 154, pp. 69–74, 2016.

[52] K. Krumova and G. Cosa, "Chapter 1: overview of reactive oxygen species," in *Singlet Oxygen: Applications in Biosciences and Nanosciences, Volume 1*, pp. 1-2, 2016.